Mon. Not. R. Astron. Soc. **000**, 1–13 (2015) Printed 16 September 2019 (MN LATEX style file v2.2)

V752 Cen - A triple-lined spectroscopic contact binary with sudden and continuous period changes

X. Zhou[1,2,3,4] ⋆, B. Soonthornthum[2], S.-B. Qian[1,3,4,5], E. Fernández, Lajús[6,7]
[1] *Yunnan Observatories, Chinese Academy of Sciences (CAS), P.O. Box 110, 650216 Kunming, China*
[2] *National Astronomical Research Institute of Thailand, 260 Moo 4, T. Donkaew, A. Maerim, Chiangmai, 50180, Thailand*
[3] *Key Laboratory of the Structure and Evolution of Celestial Objects, Chinese Academy of Sciences, P. O. Box 110, 650216 Kunming, China*
[4] *Center for Astronomical Mega-Science, Chinese Academy of Sciences, 20A Datun Road, Chaoyang District, Beijing, 100012, China*
[5] *University of the Chinese Academy of Sciences, Yuquan Road 19#, Sijingshang Block, 100049 Beijing, P. R. China*
[6] *Facultad de Ciencias Astronómicas y Geofísicas, Universidad Nacional de La Plata, Paseo del Bosque s/n, 1900, La Plata, Pcia. Bs. As., Argentina*
[7] *Instituto de Astrofísica de La Plata (CCT La plata - CONICET/UNLP), Argentina*

16 September 2019

ABSTRACT

V752 Cen is a triple-lined spectroscopic contact binary. Its multi-color light curves were obtained in the years 1971 and 2018, independently. Photometric analyses reveal that the two sets of light curves produce almost consistent results. It contains a W-subtype totally eclipsing binary, and its mass ratio and fill-out factor are $q = 3.35(1)$ and $f = 29(2)\,\%$. The absolute elements of its two component stars were determined to be $M_1 = 0.39(2)M_\odot$, $M_2 = 1.31(7)M_\odot$, $R_1 = 0.77(1)R_\odot$, $R_2 = 1.30(2)R_\odot$, $L_1 = 0.75(3)L_\odot$ and $L_2 = 2.00(7)L_\odot$. The period of V752 Cen is 0.37023198 day. The 0.37-d period remained constant from its first measurement in 1971 until the year 2000. However, it changed suddenly around the year 2000 and has been increasing continuously at a rate of $dP/dt = +5.05 \times 10^{-7} day \cdot year^{-1}$ since then, which can be explained by mass transfer from the less massive component star to the more massive one with a rate of $\frac{dM_2}{dt} = 2.52 \times 10^{-7} M_\odot/year$. The period variation of V752 Cen over the 48 years in which the period has been monitored is really unusual, and is potentially related to effects from the possible presence of a nearby third star or of a pair of stars in a second binary.

Key words: techniques: photometric — binaries: eclipsing — stars: individual (V752 Cen)

1 INTRODUCTION

Eclipsing binaries have proved to be powerful probes for studying a wide range of astrophysical problems. They are the primary sources in providing fundamental stellar parameters such as mass, radius and luminosity, which are very important in testing theoretical models of stellar evolution (Soszyński et al. 2016). Over the past decades, the number of known eclipsing binaries has increased rapidly. Photometric light curves of eclipsing binaries are archived by many survey projects, such as the Optical Gravitational Lensing Experiment (OGLE) (Graczyk et al. 2011; Rucinski 1997), the All Sky Automated Survey (ASAS) (Jayasinghe et al. 2019) and the Kepler Space Telescope (Prša et al. 2011; Slawson et al. 2011). What is even more exciting is that many spectroscopic survey projects are carried out at the same time, such as the Sloan Digital Sky Survey (SDSS) (York et al. 2000), the Large Sky Area Multi-Object Fibre Spectroscopic Telescope (LAMOST) (Qian et al. 2017, 2018) and the Gaia mission (Gaia Collaboration et al. 2016, 2018). This means that many eclipsing binaries have been observed by both photometric and spectroscopic methods.

⋆ E-mail: zhouxiaophy@ynao.ac.cn

Table 1. Newly determined mid-eclipse times.

JD (Hel.)	Error (days)	p/s	Filter	Method
2458224.6073	±0.0001	p	V	CCD
2458224.7936	±0.0001	s	V	CCD
2458225.5337	±0.0001	s	R_C	CCD
2458225.7181	±0.0001	p	R_C	CCD
2458226.6443	±0.0001	s	I_C	CCD
2458227.5692	±0.0001	p	B	CCD
2458227.7551	±0.0001	s	B	CCD
2458228.4956	±0.0001	s	V	CCD
2458228.6803	±0.0001	p	V	CCD
2458642.6058	±0.0001	p	I_C	CCD

The observations on contact binaries have a long history. Almost all identified contact binaries belong to eclipsing binaries. However, the formation of contact binaries is still an open issue. Some researchers claim that contact binaries evolve from low-mass detached close binaries via the loss of angular momentum by means of a magnetic wind (Tutukov et al. 2004; Yıldız & Doğan 2013). Another hypothesis is that tertiary components have played a very important role in the formation of contact binaries by removing angular momentum from the central binaries (Qian et al. 2013, 2014). Tertiary components are really common in contact binaries and almost every kind of celestial body can be a tertiary component orbiting the central binary, from planets to black holes (Xiao et al. 2016). Tokovinin et al. (2006) conclude that 96 % of binaries with periods shorter than 3 days have tertiary components, based on a survey of 165 solar-type spectroscopic binaries. What is more, some contact binaries even have close-in companions with distance less than 3 AU (Zhou et al. 2017), and contact binaries with more than one companions were also reported (Zhu et al. 2013; Li et al. 2015). All of these hierarchical contact binaries are very important samples for investigating the dynamic interactions among multi-stellar systems.

In 1970, Bond (1970) reported three newly discovered W UMa type contact binaries, one of which was V752 Cen (HD 101799, $V = 9.1^m$). Later, Sisteró & Castore de Sisteró (1971, 1973) observed V752 Cen photometrically and obtained UBV light curves. They claimed that V752 Cen was a completely eclipsing binary system and its components nearly filled their respective Roche lobes (a semi-detached system). The radial velocity curves of V752 Cen were also published by Sisteró & Castore de Sisteró (1974), which revealed that V752 Cen was a double-lined eclipsing binary with the spectral type of its two component stars to be F8 and F5. However, Leung (1976) claimed that V752 Cen was a contact binary with a fill-out factor of $f = 6.3\,\%$ after he reanalyzed the light curves obtained by Sisteró & Castore de Sisteró (1971, 1973). Barone et al. (1993) also supported the contact configuration with a little higher fill-out factor (9 %). The fill-out factor is defined as $f = \frac{\Omega_{in}-\Omega_{1,2}}{\Omega_{in}-\Omega_{out}}$, where Ω_{in} and Ω_{out} are the potentials at the inner and outer Lagrangian points of a binary system, and $\Omega_{1,2}$ are the surface potentials of the component stars (Ruciński 1973). The high resolution spectroscopy of V752 Cen found that it may be a triple-lined spectroscopic quadruple system (Schumacher 2009). Mallama & Pavlov (2015) pointed out that the orbital period of V752 Cen was not always constant, and there were some small magnitude changes around the time that the period was inferred to change. V752 Cen was also listed in the Gaia Data Release 2 (DR2) with effective temperature to be $T_1 = 6138K$ and parallax to be $7.96mas$ (Gaia Collaboration et al. 2016, 2018).

In the present work, we are going to reanalyze the light curves of V752 Cen published in April 1971 and the newly obtained ones in April 2018 to derive the physical parameters of the primary star and the secondary one. And also, its period variations over the past several decades will be revealed. Research on this hierarchical stellar system will provide valuable information about the evolution of hierarchical contact binary systems.

2 PHOTOMETRIC OBSERVATIONS

Photometric observations of V752 Cen were carried out at the Complejo Astronomico El Leoncito (CASLEO), San Juan, Argentina, with the 0.60 m Helen Sawyer Hogg (HSH) Telescope on 2018 April 15 - 19. Johnson-Cousins BVR_cI_c filters were used during the observations. However, only one filter was used each night. The V filter was used on 2018 April 15 and 19, and the R_c, I_c and B filters were used on 2018 April 16, 17 and 18, respectively. The observational light curves are displayed in Fig. 1. In order to get more minima times and cover a longer time span in the O - C diagram, V752 Cen was observed again with the I_c filter on 2019 June 7. A total of ten mid-eclipse times of V752 Cen were determined, which are listed in Table 1.

3 INVESTIGATION OF PERIOD VARIATIONS

Period variations commonly appear in close binary systems, especially for contact binaries, due to the possible mass transfer between their component stars or angular momentum loss from the binary systems. V752 Cen is a short period eclipsing

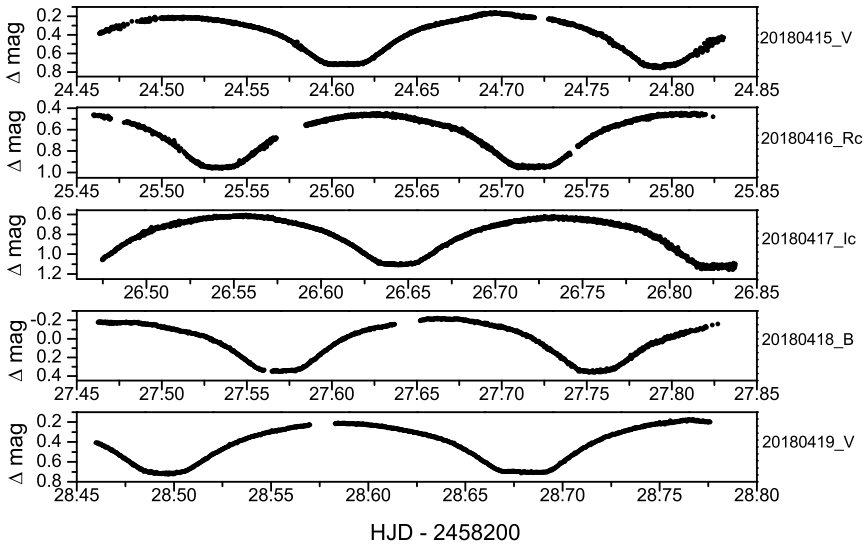

Figure 1. Observational light curves of V752 Cen. The yellow, red, green and blue colors refer to V, R_c, I_c and B filters respectively.

binary system, which is listed in the International Variable Star Index (VSX)[1] as having a period P = 0.37023198 days. In the present work, all published mid-eclipse times of V752 Cen were collected to investigate its period variations. And also, V752 Cen was observed by the SuperWASP project (Butters et al. 2010) and the Transiting Exoplanet Survey Satellite (TESS)(Ricker et al. 2015). The observational light curves were downloaded and 84 mid-eclipse times were determined from SuperWASP data. V752 Cen was observed by TESS from 2019 March 26 to 2019 April 22 continuously and 120 times of minima were determined (see Table 2). The minima in HJD were converted to BJD since the minima determined in TESS data used BJD time system. The linear equation used to calculate the $O-C$ values is:

$$Min.I(BJD) = 2456108.3448 + 0^d.37023198 \times E. \quad (1)$$

Column 1 - Heliocentric Julian Date of the observed mid-eclipse times (HJD - 2400000);
Column 2 - Barycentric Julian Date of the observed mid-eclipse times (BJD - 2400000);
Column 3 - primary (p) or secondary (s) mid-eclipse times;
Column 4 - PE, Vis and CCD refer to photoelectric, visual and Charge Coupled Device observations;
Column 5 - error of mid-eclipse times;
Column 6 - cycle numbers from the initial epoch;
Column 7 - the $O-C$ values calculated from Equation 1;
Column 8 - the references;

Table 2: Mid-eclipse times and $O-C$ values for V752 Cen (the whole table is available in the online journal).

HJD (2400000+)	BJD (2400000+)	p/s	Method	Error (days)	Epoch	$O-C$ (days)	Ref.
40648.613	40648.6135	s	PE		-41757.5	0.2306	1
40648.98393	40648.9844	s	PE		-41756.5	0.2313	2
41056.60633	41056.6068	s	PE		-40655.5	0.2283	2
41056.60640	41056.6069	s	PE		-40655.5	0.2284	2
41056.60652	41056.6070	s	PE		-40655.5	0.2285	2
41057.53144	41057.5319	p	PE		-40653	0.2278	2
41057.53191	41057.5324	p	PE		-40653	0.2283	2
41057.53220	41057.5327	p	PE		-40653	0.2286	2
41057.71732	41057.7178	s	PE		-40652.5	0.2286	2

[1] https://www.aavso.org/vsx/

Table 2 continued

HJD (2400000+)	BJD (2400000+)	p/s	Method	Error (days)	Epoch	$O-C$ (days)	Ref.
41057.71742	41057.7179	s	PE		-40652.5	0.2287	2
41057.71749	41057.7180	s	PE		-40652.5	0.2287	2
41058.64242	41058.6429	p	PE		-40650	0.2281	2
41058.64279	41058.6433	p	PE		-40650	0.2285	2
41058.64353	41058.6440	p	PE		-40650	0.2292	2
41059.56740	41059.5679	s	PE		-40647.5	0.2275	2
41059.56798	41059.5684	s	PE		-40647.5	0.2281	2
41059.56809	41059.5686	s	PE		-40647.5	0.2282	2
41059.75328	41059.7537	p	PE		-40647	0.2283	2
41059.75350	41059.7540	p	PE		-40647	0.2285	2
41059.75370	41059.7542	p	PE		-40647	0.2287	2
41060.49273	41060.4932	p	PE		-40645	0.2272	2
41060.49285	41060.4933	p	PE		-40645	0.2274	2
41060.49292	41060.4934	p	PE		-40645	0.2274	2
41060.67820	41060.6787	s	PE		-40644.5	0.2276	2
41060.67834	41060.6788	s	PE		-40644.5	0.2277	2
41060.67877	41060.6792	s	PE		-40644.5	0.2282	2
41061.60298	41061.6034	p	PE		-40642	0.2268	2
41061.60383	41061.6043	p	PE		-40642	0.2276	2
41061.60395	41061.6044	p	PE		-40642	0.2278	2
41063.63958	41063.6400	s	PE		-40636.5	0.2271	2
41063.63972	41063.6402	s	PE		-40636.5	0.2273	2
41063.63973	41063.6402	s	PE		-40636.5	0.2273	2
41064.56504	41064.5655	p	PE		-40634	0.2270	2
41064.56545	41064.5659	p	PE		-40634	0.2274	2
41064.56676	41064.5672	p	PE		-40634	0.2287	2
43244.457	43244.4576	p	Vis		-34746	0.1932	3
43245.378	43245.3786	s	Vis		-34743.5	0.1886	3
43918.649	43918.6496	p	Vis		-32925	0.1927	3
43937.533	43937.5336	p	Vis		-32874	0.1949	3
44234.616	44234.6165	s	Vis		-32071.5	0.1667	3
44235.547	44235.5476	p	Vis		-32069	0.1721	3
44243.681	44243.6816	p	Vis		-32047	0.1610	3
45428.406	45428.4066	p	Vis		-28847	0.1437	3
45430.456	45430.4566	s	Vis		-28841.5	0.1575	3
45431.372	45431.3726	p	Vis		-28839	0.1479	3
45436.357	45436.3576	s	Vis		-28825.5	0.1347	3
45438.400	45438.4006	p	Vis		-28820	0.1415	3
45753.466	45753.4666	p	Vis		-27969	0.1401	3
45804.379	45804.3796	s	Vis		-27831.5	0.1462	3
45806.391	45806.3916	p	Vis		-27826	0.1219	3
46162.362	46162.3626	s	Vis		-26864.5	0.1149	3
46163.305	46163.3056	p	Vis		-26862	0.1323	3
46164.417	46164.4176	p	Vis		-26859	0.1336	3
46166.277	46166.2776	p	Vis		-26854	0.1424	3
46167.383	46167.3836	p	Vis		-26851	0.1377	3
46530.385	46530.3857	s	Vis		-25870.5	0.1273	3
46535.379	46535.3797	p	Vis		-25857	0.1232	3
46798.595	46798.5957	p	Vis		-25146	0.1042	3
46884.321	46884.3217	s	Vis		-24914.5	0.1215	3
47262.325	47262.3257	s	Vis		-23893.5	0.1187	3
47581.452	47581.4527	s	Vis		-23031.5	0.1057	3
47663.272	47663.2727	s	Vis		-22810.5	0.1045	3
48008.319	48008.3197	s	Vis		-21878.5	0.0953	3
48373.360	48373.3607	s	Vis	0.004	-20892.5	0.0875	3
49345.583	49345.5837	s	Vis	0.005	-18266.5	0.0814	3
49773.920	49773.9207	s	Vis	0.008	-17109.5	0.0600	3
52546.3492	52546.3500	p	CCD		-9621	0.0070	4
52546.5368	52546.5375	s	CCD		-9620.5	0.0095	4
53524.1272	53524.1279	p	CCD		-6980	0.0024	4
53524.3073	53524.3080	s	CCD		-6979.5	-0.0027	4
53860.4807	53860.4814	s	CCD	0.0002	-6071.5	0.0001	5
53862.3329	53862.3327	s	CCD	0.0002	-6066.5	0.0002	5
53863.2572	53863.2579	p	CCD	0.0002	-6064	-0.0002	5

Table 2 continued

HJD (2400000+)	BJD (2400000+)	p/s	Method	Error (days)	Epoch	$O-C$ (days)	Ref.
53863.4424	53863.4432	s	CCD	0.0002	-6063.5	0	5
53864.3674	53864.3682	p	CCD	0.0002	-6061	-0.0006	5
53870.2910	53870.2918	p	CCD	0.0002	-6045	-0.0007	5
53880.2876	53880.2884	p	CCD	0.0002	-6018	-0.0004	5
53881.3981	53881.3989	p	CCD	0.0002	-6015	-0.0006	5
53886.3971	53886.3978	s	CCD	0.0002	-6001.5	0.0003	5
53887.3216	53887.3223	p	CCD	0.0003	-5999	-0.0008	5
53888.2482	53888.2489	s	CCD	0.0002	-5996.5	0.0002	5
53890.2835	53890.2842	p	CCD	0.0002	-5991	-0.0008	5
53892.3205	53892.3212	s	CCD	0.0002	-5985.5	-0.0001	5
53896.3926	53896.3933	s	CCD	0.0001	-5974.5	-0.0005	5
53897.3175	53897.3183	p	CCD	0.0001	-5972	-0.0011	5
53898.2438	53898.2445	s	CCD	0.0002	-5969.5	-0.0005	5
53902.3162	53902.3169	s	CCD	0.0001	-5958.5	-0.0006	5
53904.3517	53904.3524	p	CCD	0.0002	-5953	-0.0014	5
53905.2782	53905.2789	s	CCD	0.0002	-5950.5	-0.0005	5
53907.3135	53907.3142	p	CCD	0.0002	-5945	-0.0015	5
53910.2755	53910.2762	p	CCD	0.0002	-5937	-0.0013	5
53917.3099	53917.3107	p	CCD	0.0003	-5918	-0.0013	5
54132.5998	54132.6005	s	CCD	0.0001	-5336.5	-0.0013	5
54136.4867	54136.4875	p	CCD	0.0002	-5326	-0.0018	5
54140.5594	54140.5601	p	CCD	0.0003	-5315	-0.0017	5
54145.5585	54145.5592	s	CCD	0.0001	-5301.5	-0.0007	5
54148.5203	54148.5211	s	CCD	0.0002	-5293.5	-0.0007	5
54151.4817	54151.4825	s	CCD	0.0002	-5285.5	-0.0012	5
54153.5172	54153.5180	p	CCD	0.0002	-5280	-0.0020	5
54155.5552	54155.5559	s	CCD	0.0002	-5274.5	-0.0003	5
54159.4407	54159.4414	p	CCD	0.0002	-5264	-0.0023	5
54168.5139	54168.5146	s	CCD	0.0001	-5239.5	0.0003	5
54169.4369	54169.4376	p	CCD	0.0003	-5237	-0.0023	5
54169.6248	54169.6256	s	CCD	0.0002	-5236.5	0.0005	5
54170.3648	54170.3655	s	CCD	0.0003	-5234.5	0	5
54170.5480	54170.5487	p	CCD	0.0003	-5234	-0.0019	5
54175.3611	54175.3619	p	CCD	0.0003	-5221	-0.0018	5
54176.4718	54176.4725	p	CCD	0.0002	-5218	-0.0018	5
54178.3229	54178.3236	p	CCD	0.0003	-5213	-0.0018	5
54179.6203	54179.6210	s	CCD	0.0002	-5209.5	-0.0003	5
54180.3606	54180.3613	s	CCD	0.0002	-5207.5	-0.0004	5
54180.5442	54180.5449	p	CCD	0.0002	-5207	-0.0019	5
54181.4711	54181.4718	s	CCD	0.0001	-5204.5	-0.0006	5
54183.3222	54183.3229	s	CCD	0.0001	-5199.5	-0.0007	5
54184.4333	54184.4340	s	CCD	0.0002	-5196.5	-0.0003	5
54199.4263	54199.4271	p	CCD	0.0002	-5156	-0.0016	5
54200.3521	54200.3528	s	CCD	0.0002	-5153.5	-0.0015	5
54200.5367	54200.5375	p	CCD	0.0002	-5153	-0.0019	5
54201.2776	54201.2783	p	CCD	0.0002	-5151	-0.0016	5
54203.3139	54203.3146	s	CCD	0.0001	-5145.5	-0.0015	5
54205.3500	54205.3507	p	CCD	0.0002	-5140	-0.0017	5
54206.2758	54206.2765	s	CCD	0.0002	-5137.5	-0.0014	5
54207.3864	54207.3872	s	CCD	0.0002	-5134.5	-0.0015	5
54208.3115	54208.3122	p	CCD	0.0002	-5132	-0.0021	5
54211.2732	54211.2740	p	CCD	0.0002	-5124	-0.0022	5
54211.4592	54211.4599	s	CCD	0.0002	-5123.5	-0.0013	5
54214.4216	54214.4223	s	CCD	0.0002	-5115.5	-0.0008	5
54216.2724	54216.2731	s	CCD	0.0001	-5110.5	-0.0011	5
54225.3426	54225.3433	p	CCD	0.0002	-5086	-0.0016	5
54231.2660	54231.2667	p	CCD	0.0002	-5070	-0.0019	5
54232.3766	54232.3773	p	CCD	0.0002	-5067	-0.0020	5
54233.3038	54233.3045	s	CCD	0.0001	-5064.5	-0.0004	5
54238.3003	54238.3011	p	CCD	0.0002	-5051	-0.0020	5
54246.2616	54246.2623	s	CCD	0.0002	-5029.5	-0.0007	5
54254.2189	54254.2196	p	CCD	0.0003	-5008	-0.0034	5
54254.4052	54254.4060	s	CCD	0.0002	-5007.5	-0.0022	5
54265.3273	54265.3281	p	CCD	0.0002	-4978	-0.0019	5

Table 2 continued

HJD (2400000+)	BJD (2400000+)	p/s	Method	Error (days)	Epoch	$O-C$ (days)	Ref.
54266.2535	54266.2543	s	CCD	0.0001	-4975.5	-0.0013	5
54268.2896	54268.2904	p	CCD	0.0002	-4970	-0.0015	5
54271.2512	54271.2520	p	CCD	0.0002	-4962	-0.0017	5
54273.2883	54273.2890	s	CCD	0.0001	-4956.5	-0.0010	5
54484.5038	54484.5045	p	CCD	0.0002	-4386	-0.0028	5
54497.4625	54497.4632	p	CCD	0.0002	-4351	-0.0022	5
54499.4993	54499.5000	s	CCD	0.0001	-4345.5	-0.0017	5
54502.4609	54502.4616	s	CCD	0.0002	-4337.5	-0.0020	5
54525.4154	54525.4161	s	CCD	0.0001	-4275.5	-0.0018	5
54531.1528	54531.1536	p	CCD		-4260	-0.0030	4
54531.3398	54531.3406	s	CCD		-4259.5	-0.0011	4
54536.3364	54536.3372	p	CCD	0.0002	-4246	-0.0026	5
54564.2897	54564.2904	s	CCD	0.0001	-4170.5	-0.0019	5
54566.3250	54566.3257	p	CCD	0.0002	-4165	-0.0029	5
54569.2869	54569.2877	p	CCD	0.0002	-4157	-0.0028	5
54571.3233	54571.3241	s	CCD	0.0002	-4151.5	-0.0026	5
54579.2827	54579.2835	p	CCD	0.0002	-4130	-0.0032	5
54581.5041	54581.5048	p	CCD	0.0003	-4124	-0.0033	5
54592.2414	54592.2422	p	CCD	0.0002	-4095	-0.0026	5
54988.390	54988.3908	p	CCD	0.006	-3025	-0.0023	6
55395.277	55395.2778	p	CCD	0.005	-1926	-0.0002	7
56108.3440	56108.3448	p	CCD	0.0030	0	0	8
57051.1458	57051.1466	s	CCD	0.0002	2546.5	0.0061	4
58224.6073	58224.6081	p	CCD	0.0001	5716	0.0173	9
58224.7936	58224.7944	s	CCD	0.0001	5716.5	0.0185	9
58225.5337	58225.5345	s	CCD	0.0001	5718.5	0.0181	9
58225.7181	58225.7189	p	CCD	0.0001	5719	0.0174	9
58226.6443	58226.6451	s	CCD	0.0001	5721.5	0.0180	9
58227.5692	58227.5700	p	CCD	0.0001	5724	0.0174	9
58227.7551	58227.7559	s	CCD	0.0001	5724.5	0.0181	9
58228.4956	58228.4964	s	CCD	0.0001	5726.5	0.0182	9
58228.6803	58228.6811	p	CCD	0.0001	5727	0.0178	9
	58570.7804	p	CCD	0.0001	6651	0.0227	10
	58570.9653	s	CCD	0.0001	6651.5	0.0225	10
	58571.1507	p	CCD	0.0001	6652	0.0227	10
	58571.3356	s	CCD	0.0001	6652.5	0.0225	10
	58571.5209	p	CCD	0.0001	6653	0.0227	10
	58571.7058	s	CCD	0.0001	6653.5	0.0225	10
	58571.8911	p	CCD	0.0001	6654	0.0227	10
	58572.0761	s	CCD	0.0001	6654.5	0.0226	10
	58572.2614	p	CCD	0.0001	6655	0.0228	10
	58572.4463	s	CCD	0.0001	6655.5	0.0226	10
	58572.8165	s	CCD	0.0001	6656.5	0.0226	10
	58573.0018	p	CCD	0.0001	6657	0.0228	10
	58573.1867	s	CCD	0.0001	6657.5	0.0225	10
	58573.3720	p	CCD	0.0001	6658	0.0227	10
	58573.5570	s	CCD	0.0001	6658.5	0.0226	10
	58573.7422	p	CCD	0.0001	6659	0.0227	10
	58573.9273	s	CCD	0.0001	6659.5	0.0226	10
	58574.1125	p	CCD	0.0001	6660	0.0227	10
	58574.2975	s	CCD	0.0001	6660.5	0.0227	10
	58574.4827	p	CCD	0.0001	6661	0.0227	10
	58574.6678	s	CCD	0.0001	6661.5	0.0227	10
	58574.8529	p	CCD	0.0001	6662	0.0227	10
	58575.0380	s	CCD	0.0001	6662.5	0.0227	10
	58575.2231	p	CCD	0.0001	6663	0.0226	10
	58575.4083	s	CCD	0.0001	6663.5	0.0227	10
	58575.5933	p	CCD	0.0001	6664	0.0226	10
	58575.7785	s	CCD	0.0001	6664.5	0.0227	10
	58575.9636	p	CCD	0.0001	6665	0.0226	10
	58576.1487	s	CCD	0.0001	6665.5	0.0227	10
	58576.3338	p	CCD	0.0001	6666	0.0226	10
	58576.5189	s	CCD	0.0001	6666.5	0.0226	10
	58576.7040	p	CCD	0.0001	6667	0.0226	10

Table 2 continued

HJD (2400000+)	BJD (2400000+)	p/s	Method	Error (days)	Epoch	$O-C$ (days)	Ref.
	58576.8891	s	CCD	0.0001	6667.5	0.0220	10
	58577.0743	p	CCD	0.0001	6668	0.0226	10
	58577.2594	s	CCD	0.0001	6668.5	0.0226	10
	58577.4445	p	CCD	0.0001	6669	0.0227	10
	58577.6296	s	CCD	0.0001	6669.5	0.0226	10
	58577.8147	p	CCD	0.0001	6670	0.0226	10
	58577.9998	s	CCD	0.0001	6670.5	0.0226	10
	58578.1850	p	CCD	0.0001	6671	0.0227	10
	58578.3701	s	CCD	0.0001	6671.5	0.0226	10
	58578.5552	p	CCD	0.0001	6672	0.0226	10
	58578.7403	s	CCD	0.0001	6672.5	0.0226	10
	58578.9255	p	CCD	0.0001	6673	0.0227	10
	58579.1105	s	CCD	0.0001	6673.5	0.0226	10
	58579.2956	p	CCD	0.0001	6674	0.0226	10
	58579.4807	s	CCD	0.0001	6674.5	0.0226	10
	58579.6659	p	CCD	0.0001	6675	0.0227	10
	58579.8509	s	CCD	0.0001	6675.5	0.0226	10
	58580.0361	p	CCD	0.0001	6676	0.0227	10
	58580.2212	s	CCD	0.0001	6676.5	0.0226	10
	58580.4064	p	CCD	0.0001	6677	0.0227	10
	58580.5915	s	CCD	0.0001	6677.5	0.0226	10
	58580.7767	p	CCD	0.0001	6678	0.0227	10
	58580.9617	s	CCD	0.0001	6678.5	0.0227	10
	58581.1469	p	CCD	0.0001	6679	0.0227	10
	58581.3320	s	CCD	0.0001	6679.5	0.0227	10
	58581.5171	p	CCD	0.0001	6680	0.0227	10
	58581.7022	s	CCD	0.0001	6680.5	0.0227	10
	58584.4793	p	CCD	0.0001	6688	0.0230	10
	58584.6641	s	CCD	0.0001	6688.5	0.0228	10
	58584.8494	p	CCD	0.0001	6689	0.0229	10
	58585.0343	s	CCD	0.0001	6689.5	0.0227	10
	58585.2197	p	CCD	0.0001	6690	0.0230	10
	58585.4046	s	CCD	0.0001	6690.5	0.0227	10
	58585.5900	p	CCD	0.0001	6691	0.0230	10
	58585.7748	s	CCD	0.0001	6691.5	0.0227	10
	58585.9602	p	CCD	0.0001	6692	0.0230	10
	58586.1446	s	CCD	0.0001	6692.5	0.0223	10
	58586.3304	p	CCD	0.0001	6693	0.0230	10
	58586.5152	s	CCD	0.0001	6693.5	0.0227	10
	58586.7007	p	CCD	0.0001	6694	0.0230	10
	58586.8855	s	CCD	0.0001	6694.5	0.0227	10
	58587.0709	p	CCD	0.0001	6695	0.0230	10
	58587.2558	s	CCD	0.0001	6695.5	0.0228	10
	58587.4411	p	CCD	0.0001	6696	0.0230	10
	58587.6260	s	CCD	0.0001	6696.5	0.0228	10
	58587.8114	p	CCD	0.0001	6697	0.0230	10
	58587.9962	s	CCD	0.0001	6697.5	0.0227	10
	58588.1816	p	CCD	0.0001	6698	0.0230	10
	58588.3664	s	CCD	0.0001	6698.5	0.0227	10
	58588.5519	p	CCD	0.0001	6699	0.0230	10
	58588.7367	s	CCD	0.0001	6699.5	0.0227	10
	58588.9221	p	CCD	0.0001	6700	0.0231	10
	58589.1069	s	CCD	0.0001	6700.5	0.0228	10
	58589.2923	p	CCD	0.0001	6701	0.0230	10
	58589.4768	s	CCD	0.0001	6701.5	0.0224	10
	58589.6625	p	CCD	0.0001	6702	0.0230	10
	58589.8474	s	CCD	0.0001	6702.5	0.0228	10
	58590.0328	p	CCD	0.0001	6703	0.0230	10
	58590.2176	s	CCD	0.0001	6703.5	0.0228	10
	58590.4031	p	CCD	0.0001	6704	0.0231	10
	58590.5878	s	CCD	0.0001	6704.5	0.0227	10
	58590.7733	p	CCD	0.0001	6705	0.0231	10
	58590.9580	s	CCD	0.0001	6705.5	0.0227	10
	58591.1435	p	CCD	0.0001	6706	0.0231	10

Table 2 continued

HJD (2400000+)	BJD (2400000+)	p/s	Method	Error (days)	Epoch	$O-C$ (days)	Ref.
	58591.3283	s	CCD	0.0001	6706.5	0.0227	10
	58591.5138	p	CCD	0.0001	6707	0.0231	10
	58591.6985	s	CCD	0.0001	6707.5	0.0227	10
	58591.8840	p	CCD	0.0001	6708	0.0231	10
	58592.0687	s	CCD	0.0001	6708.5	0.0227	10
	58592.2543	p	CCD	0.0001	6709	0.0232	10
	58592.4389	s	CCD	0.0001	6709.5	0.0227	10
	58592.6245	p	CCD	0.0001	6710	0.0232	10
	58592.8092	s	CCD	0.0001	6710.5	0.0227	10
	58592.9948	p	CCD	0.0001	6711	0.0232	10
	58593.1794	s	CCD	0.0001	6711.5	0.0227	10
	58593.3650	p	CCD	0.0001	6712	0.0232	10
	58593.5497	s	CCD	0.0001	6712.5	0.0228	10
	58593.7352	p	CCD	0.0001	6713	0.0232	10
	58593.9199	s	CCD	0.0001	6713.5	0.0228	10
	58594.1055	p	CCD	0.0001	6714	0.0232	10
	58594.2902	s	CCD	0.0001	6714.5	0.0228	10
	58594.4757	p	CCD	0.0001	6715	0.0231	10
	58594.6605	s	CCD	0.0001	6715.5	0.0228	10
	58594.8460	p	CCD	0.0001	6716	0.0232	10
	58595.0307	s	CCD	0.0001	6716.5	0.0228	10
	58595.2162	p	CCD	0.0001	6717	0.0232	10
	58595.4009	s	CCD	0.0001	6717.5	0.0228	10
	58595.5864	p	CCD	0.0001	6718	0.0231	10
58642.6058	58642.6066	p	CCD	0.0001	6845	0.0239	9

References: (1) Bond (1970); (2) Sisteró & Castore de Sisteró (1973); (3) BBSAG Bulletins[2]; (4) Mallama & Pavlov (2015); (5) SuperWASP[3]; (6) Paschke (2009); (7) Paschke (2010); (8) Paschke (2013); (9) The present work; (10) TESS.

The $O-C$ values calculated with Equation 1 are displayed in Fig. 2 with solid circles. The solid circles are split into two parts since the period of V752 Cen seems to change suddenly around the year 2000. Its period was constant during the first 30 years after it was first reported by Bond (1970), as displayed in the upper panel in Fig. 2. The new linear equation is:

$$Min.I(BJD) = 2456108.2896(\pm 0.0002) + 0^d.370225027(\pm 0.000000005) \times E. \quad (2)$$

The second part of the $O-C$ values as shown in the lower part of Fig. 2, is increasing continuously from the year 2000 up to the present day. Thus, a quadratic term is superposed on the initial linear Equation 1. The new ephemeris is:

$$\begin{aligned} Min.I(BJD) &= 2456108.3443(\pm 0.0001) + 0^d.370233636(\pm 0.000000004) \times E \\ &+2.56(\pm 0.02) \times 10^{-10} \times E^2. \end{aligned} \quad (3)$$

The fitting of the observed O - C data reveals that the period of V752 Cen changed suddenly around the year 2000. Since then, it has been increasing continuously at a rate of $dP/dt = +5.05 \times 10^{-7} day \cdot year^{-1}$ ($+0.044s \cdot year^{-1}$). To illustrate the sudden period change more clearly, the O - C curve for the whole time span is shown in Fig. 3. It should be mentioned that we have tried to fit the observed O - C data with other possibilities, for example, orbital motion of the contact binary in a long-period elliptical orbit. However, the latter possibility would require the presence of a star (or stars) with an implausibly high mass (masses), so it was dropped from further consideration.

4 MODELING THE LIGHT CURVES

The light curves were obtained in April, 1971. The newly observed light curves displayed in Fig. 1 were obtained in April, 2018. The two sets of light curves are modeled with the Wilson-Devinney (W-D) program (Wilson 2012; Wilson & Van Hamme 2014). The light curves show that V752 Cen is a totally eclipsed W UMa system. Mode 3 for contact binary is chosen, and the q-search method is not necessary (Terrell & Wilson 2005). The mean surface temperature is given as $T_1 = 6138K$ in the Gaia DR2 with a typical error of 324K (Andrae et al. 2018). Sisteró & Castore de Sisteró (1974) reported that the spectral type of the primary star is F8, corresponding to a temperature of 6250K (Cox 2000). The spectral types derived from B - V and J - H were G0 and F7, respectively. We adopted the temperature from the Gaia DR2 since the uncertainty of about 300K in temperature will not significantly change parameters like mass ratio, orbital inclination and fill-out factor (Jiang et al. 2015;

[2] https://www.astronomie.info/bbsag/bulletins.html
[3] https://wasp.cerit-sc.cz/form

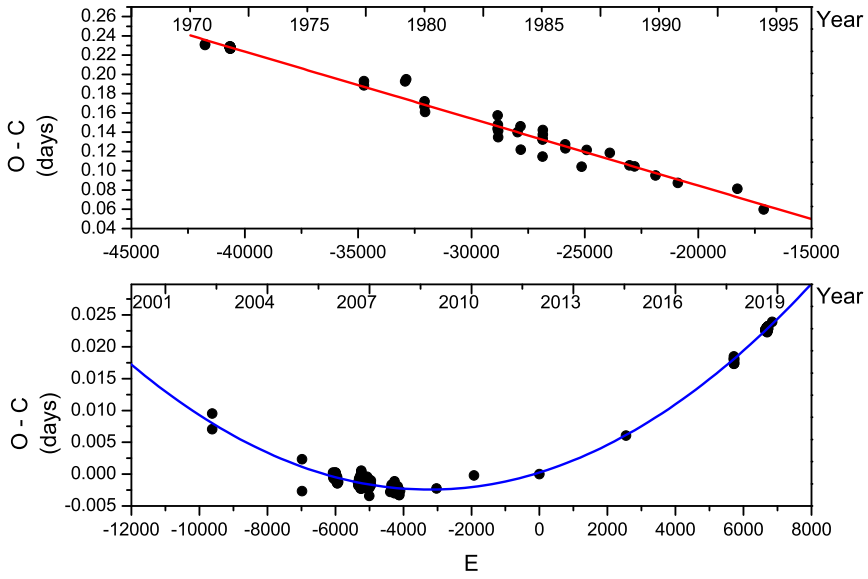

Figure 2. In both panels, the solid circles are O-C values calculated from Equation 1. In the upper panel, the red line represents, relative to Equation 1, the expected O-C curve based on Equation 2. In the lower panel, the blue curve represents, relative to Equation 1, the expected O-C curve based on Equation 3.

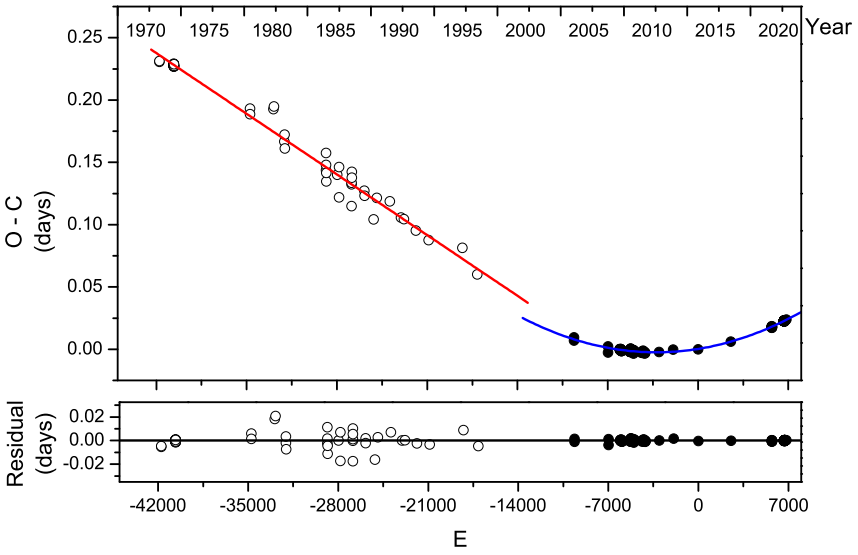

Figure 3. The O - C curve for the whole 48 - year interval.

Zhou et al. 2015). The gravity-darkening coefficients and bolometric albedo coefficients are set at $g_1 = g_2 = 0.32$ (Lucy 1967) and $A_1 = A_2 = 0.5$ (Ruciński 1969), respectively, and the limb darkening coefficients are set accordingly (Van Hamme 1993). The star eclipsed at primary minimum is assumed to be the primary star. The adjustable parameters are the mass ratio (q), orbital inclination (i), modified dimensionless surface potential of the primary star (Ω_1), mean surface temperature of the secondary star (T_2), bandpass luminosities of the primary star (L_1), and spots' parameters. The determined photometric parameters are listed in Table 3. The theoretical light curves based on the Roche model are displayed in Fig. 4 and Fig. 5. The U and B band light curves are shifted vertically by 0.3 and 0.1 mag in Fig. 4. The V band light curves observed on 19 April 2018 are shifted vertically by -0.2 mag in Fig. 5.

Table 3. Photometric solutions for V752 Cen

Parameters	Data 1971	Data 2018
$T_1(K)$	6138(fixed)	6138(fixed)
q (M_2/M_1)	3.31(±0.02)	3.35(±0.01)
$i(^\circ)$	81.8(±0.2)	82.07(±0.06)
Ω_{in}	7.02	7.08
Ω_{out}	6.40	6.45
$\Omega_1 = \Omega_2$	6.85(±0.02)	6.89(±0.01)
$T_2(K)$	5947(±7)	6014(±2)
$\Delta T(K)$	191	124
T_2/T_1	0.969(±0.001)	0.9798(±0.0003)
$L_1/(L_1+L_2)$ (U)	0.305(±0.001)	
$L_1/(L_1+L_2)$ (B)	0.296(±0.001)	0.2798(±0.0003)
$L_1/(L_1+L_2)$ (V)	0.286(±0.001)	0.2735(±0.0003)
$L_1/(L_1+L_2)$ (V)		0.2735(±0.0002)
$L_1/(L_1+L_2)$ (R_c)		0.2706(±0.0003)
$L_1/(L_1+L_2)$ (I_c)		0.2683(±0.0003)
$r_1(pole)$	0.2733(±0.0005)	0.2730(±0.0003)
$r_1(side)$	0.2862(±0.0006)	0.2861(±0.0003)
$r_1(back)$	0.3289(±0.0011)	0.3295(±0.0004)
$r_2(pole)$	0.4664(±0.0020)	0.4676(±0.0008)
$r_2(side)$	0.5045(±0.0028)	0.5059(±0.0012)
$r_2(back)$	0.5336(±0.0038)	0.5351(±0.0016)
f	27 %(±4 %)	29 %(±2 %)
$\theta(^\circ)$	155.6(±0.6)	153.7(±1.1)
$\psi(^\circ)$	240.5(±2.7)	278.6(±0.5)
r(rad)	0.53(fixed)	0.53(fixed)
T_f	0.73(fixed)	0.73(fixed)
$\Sigma\omega(O-C)^2$	0.00256	0.00260

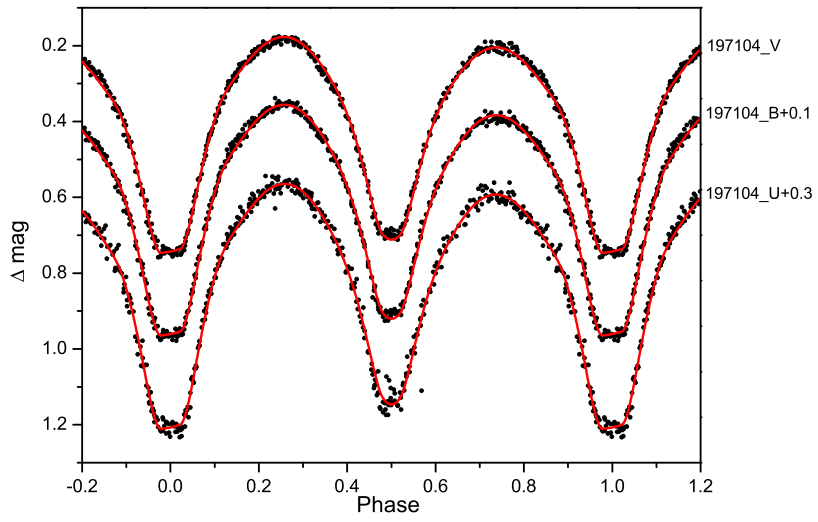

Figure 4. The solid circles are the U, B and V band light curves observed in April 1971 and the red lines are the corresponding theoretical light curves.

5 DISCUSSION AND CONCLUSION

According to the photometric solutions in Table 3, the light curves observed in 1971 and 2018 provide almost consistent results. The two component stars and geometric structure of V752 Cen were quite stable over the past forty-eight years. The solutions show that V752 Cen is a W-subtype contact binary sytem. The star eclipsed at primary minimum is hotter but less massive than the star eclipsed at secondary minimum. The orbital inclination is $i(^\circ) = 82.07$, and the totally

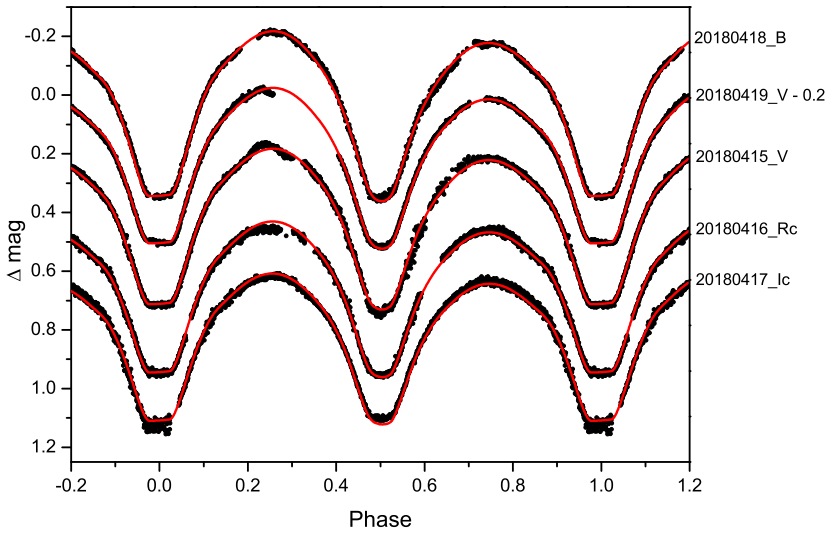

Figure 5. The solid circles are the B, V, $R_c$and I_c band light curves observed in April 2018 and the red lines are the corresponding theoretical light curves.

Table 4. Absolute parameters of components in V752 Cen

Parameters	Primary	Secondary
M	$0.39(\pm0.02)M_\odot$	$1.31(\pm0.07)M_\odot$
R	$0.77(\pm0.01)R_\odot$	$1.30(\pm0.02)R_\odot$
L	$0.75(\pm0.03)L_\odot$	$2.00(\pm0.07)L_\odot$

eclipsed characteristic implies that the determined parameters are very reliable. Considering the mass function obtained by Sisteró & Castore de Sisteró (1974): $(M_1+M_2)sin^3i = 1.648\pm0.089M_\odot$, the absolute parameters of the two component stars are calculated and listed in Table 4. The orbital semi-major axis is calculated to be $a = 2.59(\pm0.05)R_\odot$. It should be mentioned that the mass ratio of V752 Cen was determined to be $q = 0.31$ from spectroscopic observations (Sisteró & Castore de Sisteró 1974), which was similar to our value ($1/3.35 = 0.30$).

V752 Cen is a triple-lined spectroscopic quadruple system, and the tertiary and fourth components may make up a far away binary system (Schumacher 2009). We have also tried to set third light (l_3) as a free parameter while modeling the light curve with the W - D program. However, the solution is not convergent. It means that the potential binary orbiting around V752 Cen should be late-type stars and don't contribute any light to the light curves of V752 Cen. The period analysis of V752 Cen reveals that its period was constant from 1970 to 2000, which means there was no mass transfer between the two component stars during that time interval. Then, its period changed suddenly around the year 2000. However, photometric analysis implies that the component stars in central binary system are very stable. Thus, the sudden period change may have been caused by the interaction between V752 Cen and the potential binary that is orbiting it. The period of V752 Cen has been increasing continuously at a rate of $dP/dt = +5.05\times10^{-7}day\cdot year^{-1}$ ($+0.044s\cdot year^{-1}$) after that sudden period change happened. The period change is almost the same as that determined by Lohr et al. (2015), which was $+0.04379s\cdot year^{-1}$. It can be explained by mass transfer from the less massive component star to the more massive one, and the mass transfer rate is estimated to be $\frac{dM_2}{dt} = 2.52\times10^{-7}M_\odot/year$.

Both spectroscopic and photometric observations have indicated that many contact binaries are accompanied by at least one additional companion (Pribulla & Rucinski 2006; Rappaport et al. 2013). Therefore, hierarchical contact binary systems are probably common. What is more important is that all short period M-dwarf contact binaries may have additional companions since the time-scale of angular momentum loss for the components is too long (Stępień 2011). Naoz & Fabrycky (2014) claim that the eccentric Kozai-Lidov mechanism may remove angular momentum from central binaries and result in tidal tightening of inner binaries in triple star systems. However, no observational evidence on dynamic interactions between inner binaries and additional companions was reported. In that respect, V752 Cen is a very interesting hierarchical contact binary system with significant research value. The research on its light curves and period variations suggests that dynamic interactions may have happened between the inner binary and companion stars orbiting it. However, more observations and

analyses on hierarchical contact binary systems are still needed to investigate the dynamic mechanism between the central binary and its companion stars in detail.

ACKNOWLEDGEMENTS

We appreciate the valuable comments and suggestions from the anonymous referee. We are grateful to Professor Wayne Orchiston for improving the manuscript. This research was supported by the National Natural Science Foundation of China (Grant No. 11703080 and 11703082), the Joint Research Fund in Astronomy (Grant No. U1931101) under cooperative agreement between the National Natural Science Foundation of China and Chinese Academy of Sciences, and the Yunnan Natural Science Foundation (Grant No. 2018FB006 and 2016FB004). It was part of the research activities at the National Astronomical Research Institute of Thailand (Public Organization). This work has made use of data from the European Space Agency (ESA) mission *Gaia*, processed by the *Gaia* Data Processing and Analysis Consortium (DPAC). Funding for the DPAC has been provided by national institutions, in particular the institutions participating in the *Gaia* Multilateral Agreement. This paper makes use of data from the DR1 of the WASP data as provided by the WASP consortium, and the computing and storage facilities at the CERIT Scientific Cloud, reg. no. CZ.1.05/3.2.00/08.0144 which is operated by Masaryk University, Czech Republic.

REFERENCES

Andrae, R., Fouesneau, M., Creevey, O., et al. 2018, A&A, 616, A8
Barone, F., di Fiore, L., Milano, L., & Russo, G. 1993, ApJ, 407, 237
Butters, O. W., West, R. G., Anderson, D. R., et al. 2010, A&A, 520, L10
Bond, H. E. 1970, PASP, 82, 1065
Cox, A. N. 2000, Allen′s Astrophysical Quantities (4th ed.; NewYork: Springer)
D'Angelo, C., van Kerkwijk, M. H., & Rucinski, S. M. 2006, AJ, 132, 650.
Gaia Collaboration, Prusti, T., de Bruijne, J. H. J., et al. 2016, A&A, 595, A1
Gaia Collaboration, Brown, A. G. A., Vallenari, A., et al. 2018, A&A, 616, A1
Graczyk, D., Soszyński, I., Poleski, R., et al. 2011, Acta Astron., 61, 103
Jayasinghe, T., Stanek, K. Z., Kochanek, C. S., et al. 2019, MNRAS, 486, 1907
Jiang, L.-Q., Qian, S.-B., Zhang, J., et al. 2015, AJ, 149, 169
Leung, K.-C. 1976, PASP, 88, 936
Li, K., Hu, S.-M., Guo, D.-F., et al. 2015, AJ, 149, 120
Lohr, M. E., Norton, A. J., Payne, S. G., et al. 2015, A&A, 578, A136
Lucy, L. B. 1967, ZAp, 65, 89
Mallama, A., & Pavlov, H. 2015, Journal of the American Association of Variable Star Observers (JAAVSO), 43, 38
Naoz, S., & Fabrycky, D. C. 2014, ApJ, 793, 137
Paschke, A. 2009, Open European Journal on Variable Stars, 116, 1
Paschke, A. 2010, Open European Journal on Variable Stars, 130, 1
Paschke, A. 2013, Open European Journal on Variable Stars, 155, 1
Pribulla, T., & Rucinski, S. M. 2006, AJ, 131, 2986
Prša, A., Batalha, N., Slawson, R. W., et al. 2011, AJ, 141, 83
Qian, S.-B., Liu, N.-P., Li, K., et al. 2013, ApJS, 209, 13
Qian, S.-B., Zhou, X., Zola, S., et al. 2014, AJ, 148, 79
Qian, S.-B., He, J.-J., Zhang, J., et al. 2017, Research in Astronomy and Astrophysics, 17, 87
Qian, S.-B., Zhang, J., He, J.-J., et al. 2018, ApJS, 235, 5
Rappaport, S., Deck, K., Levine, A., et al. 2013, ApJ, 768, 33
Ricker, G. R., Winn, J. N., Vanderspek, R., et al. 2015, Journal of Astronomical Telescopes, Instruments, and Systems, 1, 014003
Ruciński, S. M. 1969, AcA, 19, 245
Ruciński, S. M. 1973, Acta Astron., 23, 79
Rucinski, S. M. 1997, AJ, 113, 1112
Schumacher, H. 2009, The Eighth Pacific Rim Conference on Stellar Astrophysics: A Tribute to Kam-Ching Leung, 404, 199
Sisteró, R. F., & Castore de Sisteró, M. E. 1974, AJ, 79, 391
Sisteró, R. F., & Castore de Sisteró, M. E. 1973, AJ, 78, 413
Sisteró, R. F., & Castore de Sisteró, M. E. 1971, Information Bulletin on Variable Stars, 576, 1
Slawson, R. W., Prša, A., Welsh, W. F., et al. 2011, AJ, 142, 160.

Soszyński, I., Pawlak, M., Pietrukowicz, P., et al. 2016, Acta Astron., 66, 405
Stępień, K. 2011, Acta Astron., 61, 139
Terrell, D., & Wilson, R. E. 2005, Ap&SS, 296, 221
Tokovinin, A., Thomas, S., Sterzik, M., et al. 2006, A&A, 450, 681
Tutukov, A. V., Dremova, G. N., & Svechnikov, M. A. 2004, Astronomy Reports, 48, 219
Van Hamme, W. 1993, AJ, 106, 2096
Wilson, R. E. 2012, AJ, 144, 73
Wilson, R. E., & Van Hamme, W. 2014, ApJ, 780, 151
Yıldız, M., & Doğan, T. 2013, MNRAS, 430, 2029
Xiao, Z., Shengbang, Q., Binghe, H., et al. 2016, PASJ, 68, 102
York, D. G., Adelman, J., Anderson, J. E., et al. 2000, AJ, 120, 1579
Zhou, X., Qian, S.-B., Liao, W.-P., et al. 2015, AJ, 150, 83
Zhou, X., Qian, S., & Zhang, B. 2017, PASJ, 69, 37
Zhu, L. Y., Qian, S. B., Liu, N. P., Liu, L., & Jiang, L. Q. 2013, AJ, 145, 39